Carbohydrate Polymers 101 (2014) 104–112

Contents lists available at ScienceDirect

Carbohydrate Polymers

journal homepage: www.elsevier.com/locate/carbpol

Design and formulation of trimethylated chitosan-graft-poly(ε-caprolactone) nanoparticles used for gene delivery

San Tang, Zhixiong Huang, Haiwen Zhang, Youxiang Wang*, Qiaoling Hu, Hongliang Jiang*

MOE Key Laboratory of Macromolecular Synthesis and Functionalization, Department of Polymer Science and Engineering, Zhejiang University, Hangzhou 310027, PR China

ARTICLE INFO

Article history:
Received 12 March 2013
Received in revised form 3 September 2013
Accepted 16 September 2013
Available online 19 September 2013

Keywords:
Trimethylated chitosan
Poly(ε-caprolactone)
Nanoparticles
Non-viral gene delivery

ABSTRACT

The ideal gene polyplexes should have a subtle balance between polyplex stability to protect DNA against nucleases, and polyplex instability to permit DNA dissociation inside cells. In this research, low molecular weight trimethylated chitosan was chemically modified with poly(ε-caprolactone). Owing to the amphiphilic character, trimethylated chitosan-graft-poly(ε-caprolactone) (TMC-g-PCL) formed nanoparticles in aqueous media. TMC-g-PCL nanoparticles could effectively condense pDNA into polyplexes about 200 nm in size. The TMC-g-PCL/DNA polyplexes were stable in physiological salt condition and showed high uptake efficiency probably due to the increasing cell membrane-carrier interaction as a result of hydrophobic modification. However, the high degree of quaternization influenced the buffer capacity of TMC-g-PCL and led to a reduction in the release from the lysosomes. By adding chloroquine to exclude the limitation of lysosome escape, the transfection efficiency of TMC-g-PCL/DNA polyplexes was similar to that of PEI/DNA polyplexes. This study demonstrated the potential of TMC-g-PCL/DNA nanoparticles as an efficient carrier for gene delivery.

1. Introduction

Gene therapy is considered as a promising approach for the treatment of congenital and acquired diseases by producing bioactive agents or preventing abnormal functions of the cells such as genetic disorder or uncontrollable proliferation of cells (Kim & Rossi, 2007; O'Connor & Crystal, 2006). Non-viral vectors, including cationic lipids and polycations that can associate with negatively charged DNA, have recently emerged as viable alternative due to the lower cost of synthesis, lack of an immune response and large nucleic acid loading capacity (Itaka & Kataoka, 2009; Maji et al., 2012; Peng, Chen, Zhong, & Zhuo, 2010; Ren, Ji, & Shen, 2005; Wang, Zhu, Hu, & Shen, 2008; Yu et al., 2007).

Chitosan (CS) is well known as a biocompatible, biodegradable and low toxicity material with high cationic potential and has been widely applied in gene delivery (Lee, Kwon, Kim, Jo, & Jeong, 1998; Liu et al., 2005; Lu et al., 2009; Pires et al., 2011). High molecular weight chitosan (100–400 kDa) can form extremely stable polyplexes with DNA (Koping-Hoggard et al., 2004). However, some problems, such as poor solubility at physiological pH value, high viscosity at concentrations used for in vivo delivery and a slow dissociation and release of plasmid DNA inside the cells, limited the successful applications of chitosan-mediated gene delivery (Germershaus, Mao, Sitterberg, Bakowsky, & Kissel, 2008; Varum, Ottoy, & Smidsrod, 1994). Chitosan oligomers with molecular weight lower than 5000 Da are water soluble at physiological pHs. However, due to the weak interaction with DNA, the polyplexes were physically unstable and thus transfected cells at low efficiency (Köping-Höggård, Mel'nikova, Vårum, Lindman, & Artursson, 2003). To overcome these drawbacks, many chitosan derivatives have been developed in the last few years. A cationized chitosan derivative N,N,N-trimethyl chitosan chloride (TMC), which shows higher solubility at physiological pHs, has been synthesized as gene vector. The degree of quaternization and the molecular weight of TMC play important roles in its gene transfection efficiency and cytotoxicity (Mao et al., 2005). TMC with high molecular weight and high degree of quaternization shows strong cytotoxicity in vitro cell culture experiment (Kean, Roth, & Thanou, 2005). The strong electrostatic interaction between TMC and DNA impeded gene dissociation inside cells, thus lead to low transfection. Therefore, further improvement of the gene delivery efficiency and biocompatibility of TMC is also urgently required.

Much progress has been made by grafting hydrophilic (Germershaus, Mao, Sitterberg, Bakowsky, & Kissel, 2008; Park et al., 2000), hydrophobic (Chae, Son, Lee, Jang, & Nah, 2005; Liu et al., 2003), or cell-specific side chains (Cook et al., 2005; Lee, Lockey, & Mohapatra, 2006; Mansouri et al., 2006) to chitosan or TMC backbones. Among them, hydrophobic group-modified

* Corresponding authors. Tel.: +86 571 87953729; fax: +86 571 87953729.
E-mail addresses: yx_wang@zju.edu.cn (Y. Wang), hljiang@zju.edu.cn (H. Jiang).

0144-8617/$ – see front matter © 2013 Elsevier Ltd. All rights reserved.
http://dx.doi.org/10.1016/j.carbpol.2013.09.053

chitosans have been widely investigated with respect to enhanced gene transfection efficiency. Alkylated chitosans were prepared by modifying chitosan with alkyl (butyl, octyl, dodecyl, or hexadecyl) bromide and showed increased transfection efficiency on C2C12 mouse myoblast cell lines (Liu, De Yao, & Liu, 2001; Liu et al., 2003). The reason was that the hydrophobic chains promoted the cell uptake and the unpacking of genes from the vectors. Deoxycholic acid-conjugated chitosan oligosaccharide nanoparticles showed superior gene condensation and protection of the condensed gene from endonuclease attack compared with unmodified chitosan oligosaccharides. Moreover, it showed high level of gene transfection efficiencies on HEK 293 cells, even in the presence of serum (Chae, Son, Lee, Jang, & Nah, 2005). Hydrophobic stearic acid (Hu et al., 2006), 5β-cholanic acid (Sang Yoo, Eun Lee, Chung, Chan Kwon, & Young Jeong, 2005), cholesterol (Son et al., 2004) was also used to modify chitosan to construct efficient gene delivery systems.

Poly(ε-caprolactone) (PCL) is an aliphatic polyester, often used in biomedical applications because of its biocompatibility, slow biodegradability, low-cost, non-toxicity and good mechanical properties (Drevelle, Daviau, Lauzon, & Faucheux, 2013; Wei et al., 2009). In this research, trimethylated chitosan with molecular weight about 15 kDa was chosen and then grafted by PCL (TMC-g-PCL) as gene vector. The introduction of hydrophobic PCL moieties into TMC could induce the amphiphilicity-driven self association, which resulted in the formation of nanoparticles in an aqueous media. The TMC shell might offer efficient gene condensation capacity with reduced cytotoxicity due to the low molecular weight of TMC. The hydrophobic interaction between PCL chain and cell membrane might facilitate the TMC-g-PCL/DNA polyplexes enter into the cells. And the hydrophobicity-induced weakening of the electrostatic attraction between DNA and carriers might lead to the easier unpacking of DNA inside the cells and increase the transfection (Liu et al., 2003). We investigated the chemo-physical properties of TMC-g-PCL/DNA polyplexes, featuring their utility as gene delivery systems under serum-containing conditions.

2. Materials and methods

2.1. Materials

Chitosan was purchased from Yuhuan Ocean Biomaterial Co. (Yuhuan, China). The degree of deacetylation (DD) was found to be 91.5% by ^{1}H NMR analysis and the viscosity-average molecular weight was determined to be 1.5×10^4. PCL (Mn 6200) was synthesized in our laboratory using benzyl alcohol as an initiator and $Sn(OCt)_2$ as a catalyst. Formaldehyde, formic acid, and iodomethane were obtained from Shanghai Chemical Company (Shanghai, China). Sodium dodecyl sulfate (SDS) was obtained from Shantou Xilong Chemical Company (Shantou, China). Hexamethylene diisocyanate (HDI) was supplied by Acros (Shanghai, China). Tin (II) dibutyl dilaurate and tris(hydroxymethyl)aminomethane (Tris) were purchased from Sinopharm Chemical Reagent Co (Shanghai, China). Trifluoroethanol was from Weihai New Era Chemical Co (Weihai, China). 3-(4,5-Dimethylthiazol-2-yl)-2,5-diphenyltetrazolium bromide (MTT), fluorescein isothiocyanate (FITC), polyethylenimine (branched, M_w 25 kDa), 4,6-diamidino-2-phenylindole (DAPI) and chloroquine were purchased from Sigma–Aldrich. FITC-DNA was synthesized according to the literature (Sato, Kawakami, Shirakawa, & Okahata, 1995). Deoxyribonucleic acid (DNA, fish sperm, sodium salt) and N-[2-hydroxyethyl] piperazine-N′-[2-ehtanesulfonic acid] (HEPEs) were purchased from AMRESCO. Lyso Tracker® Red DND-99 was purchased from Dawen Biotec. pEGFP (4733 bp) was purchased from Clonetech. The fish sperm DNA was chosen as model DNA to measure the particle size, zeta potential and morphology of polyplexes. pEGFP was used in gel retardation assay and cell culture. All other chemicals and solvents were of analytical grade and used as received.

2.2. Synthesis and characterization of TMC-g-PCL

Trimethylated chitosan-g-poly(ε-caprolactone) was synthesized according to the literature (Zhang, Cai, Tang, Wang, & Jiang, 2011). N,N-dimethylated chitosan (DMC) was first synthesized following the procedures described by Verheul et al. (2008). Then, sodium dodecyl sulfate (SDS)-DMC complex (SDC) was prepared simply by mixing acidic solutions of DMC and SDS (Cai, Jiang, Tu, Wang, & Zhu, 2009). The mixture was gently stirred for 2 h at room temperature. The resulting SDC precipitates were collected by centrifugation and washed three times with distilled water and finally freeze-dried to yield yellowish powders. Hydroxyl-terminated PCL was activated by HDI to yield PCL-NCO (Folmer, Sijbesma, Versteegen, van der Rijt, & Meijer, 2000). SDC was dissolved in anhydrous DMSO. Then, PCL-NCO dissolved in anhydrous $CHCl_3$ was added to SDC solution to yield DMC-g-PCL by coupling reaction (Zhang, Cai, Tang, Wang, & Jiang, 2011). DMC-g-PCL was further reacted with iodomethane, isolated by centrifugation and washed extensively with ethyl ether. After drying overnight, the crude TMC-g-PCL was dissolved in 5 mL of DMSO. 30 mL of 15% NaCl solution was added. The mixture was stirred for at least 18 h for ion-exchange, followed by dialysis against deionized water for 3 days with a cellulose membrane (M_w cut off 3500). The deionized water was changed twice a day. The final product was obtained by freeze drying. TMC-g-PCL was characterized by ^{1}H NMR (Bruker DMX-500 NMR spectrometer).

The critical aggregation concentration (CAC) was determined according to the literature (Lim Soo, Luo, Maysinger, & Eisenberg, 2002). Pyrene was used as a hydrophobic fluorescence probe to analyze the self-assembly of TMC-g-PCL in pH 7.4 HEPEs buffer solution. The concentration of TMC-g-PCL was ranged from 1.0×10^{-3} to 1.0 mg/ml. The pyrene concentration was 6.0×10^{-7} M. Pyrene excitation spectra were recorded on a HITACHIF-4500 fluorescence spectrophotometer (Hitachi High Technologies Corporation, Tokyo, Japan). The slit widths for both excitation and emission sides were maintained at 3 nm and an emission wavelength of 373 nm was used.

2.3. Preparation of TMC-g-PCL nanoparticles

The nanoparticles were prepared by a dialysis procedure described by Lim Soo, Luo, Maysinger, and Eisenberg (2002). Briefly, TMC-g-PCL copolymer (0.025 g) was first dissolved in 6 ml of trifluoroethanol/acetic acid (v/v, 5/1) admixture. Then the solution was dialyzed against distilled water with a cellulose membrane (M_w cut off 3500) at room temperature for 3 days to yield a transparent solution. The resulting solvent-free solution was then filtered with 0.45 μm filter and diluted with HEPEs buffer solution to give a copolymer concentration of 1.0 mg/ml.

2.4. Preparation and characterization of TMC-g-PCL/DNA polyplexes

DNA was dissolved in HEPES (pH 7.4, 20 mM NaCl) to give a concentration of 0.1 mg/ml. Different concentrations of the TMC-g-PCL nanoparticles were added to a constant volume of DNA solution to obtain various weight ratios (carrier/DNA) ranging from 4 to 30. The mixture was vortexed for 15 s and incubated for 30 min at room temperature to ensure polyplex formation. For convenience, the TMC-g-PCL/DNA polyplexes at weight ratios of 12 was marked as TMC-g-PCL/DNA-12.

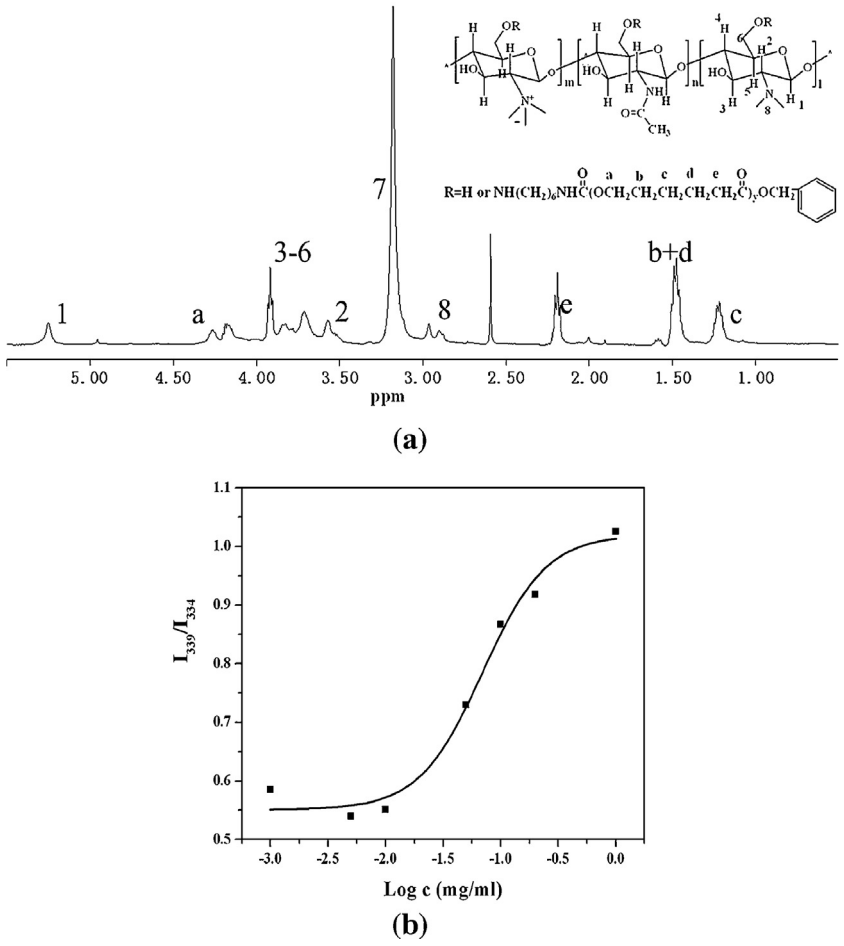

Fig. 1. (a) ^{1}H NMR spectra of TMC-g-PCL in CF_3COOD/D_2O (v/v, 1/2) and (b) plots of the I_{339}/I_{334} ratio of pyrene excitation spectra in pH 7.4 HEPES as a function of TMC-g-PCL concentration.

Particle size measurement was performed by dynamic light scattering (DLS, 90plus/BI-MAS particle size analyzer, Holtsville, USA), which detected at 90° angle and determined at 25 °C. Every measurement was repeated 4 times. The zeta potential was measured using the Zetasizers 3000 (Malvern Instruments, Southborough, MA). The morphology of TMC-g-PCL nanoparticles and gene polyplexes was conducted by transmission electron microscope (TEM, JEM-1200EX, NEC, Japan) operated at 50 kV. A drop of the nanoparticles was deposited onto 200-mesh carbon-coated copper grid for 10 min. The excess aqueous solution was blotted with filter paper. In order to obtain enough particles on the grid, the above processes were repeated three times. The DNA binding ability of polyplexes was examined by gel retardation assay according to the literature (Li et al., 2011). The polyplexes were electrophoresed through a 1% agarose gel at 100 V for 50 min, then the gel was stained with ethidium bromide (0.5 μg/mL) for 30 min and DNA was visualized on a UV transilluminator.

2.5. Aggregation study of polyplexes

All polyplexes were prepared as mentioned above. Then the NaCl concentration was adjusted to 150 mM, which was comparable to the physiological salt condition. The colloidal stability was investigated by DLS according to the time-depended particle size. The stability of TMC-g-PCL/DNA polyplexes in complete DMEM medium containing 10% fetal bovine serum (FBS) was also evaluated by DLS.

2.6. Cell culture

The human embryonic kidney cell line HEK293T was cultured with complete medium (DMEM containing 10% FBS, supplemented with 100 U/ml penicillin G and 100 μg/ml streptomysin). Then, the cells were maintained at 37 °C in a humid atmosphere containing 5% CO_2.

2.6.1. Cytotoxicity of TMC-g-PCL/DNA polyplexes

The MTT assay is a non-radio-active colorimetric assay to measure cytotoxicity (Mosmann, 1983). HEK293T cells were seeded at a density of 1×10^4 cells per well in 96-well tissue culture polystyrenes (TCPS) plate and incubated for 24 h in the 5% CO_2 incubator. Then TMC-g-PCL/DNA and PEI/DNA polyplexes at the same weight ratio containing 1 μg DNA were added respectively. After incubation for 24 h, 20 μL of MTT solution (5 mg/mL in PBS) was added to each well and incubated for additional 4 h. Then the medium was removed and DMSO was added. The plates were mildly shaken for 10 min to ensure the dissolution of formazan. The absorbance values were measured by using microplate reader (Bio-RAD, model 550) at wavelength 570 nm, blanked with DMSO solution. PEI/DNA polyplexes were used as a control. All experiments were performed in five replicates. Error bars represent means ± standard deviation (SD) for $n = 5$.

2.6.2. Cell uptake

HEK293T cells were seeded in 24-well tissue culture plates at a density of 1×10^5 cells per well and incubated for 24 h. The

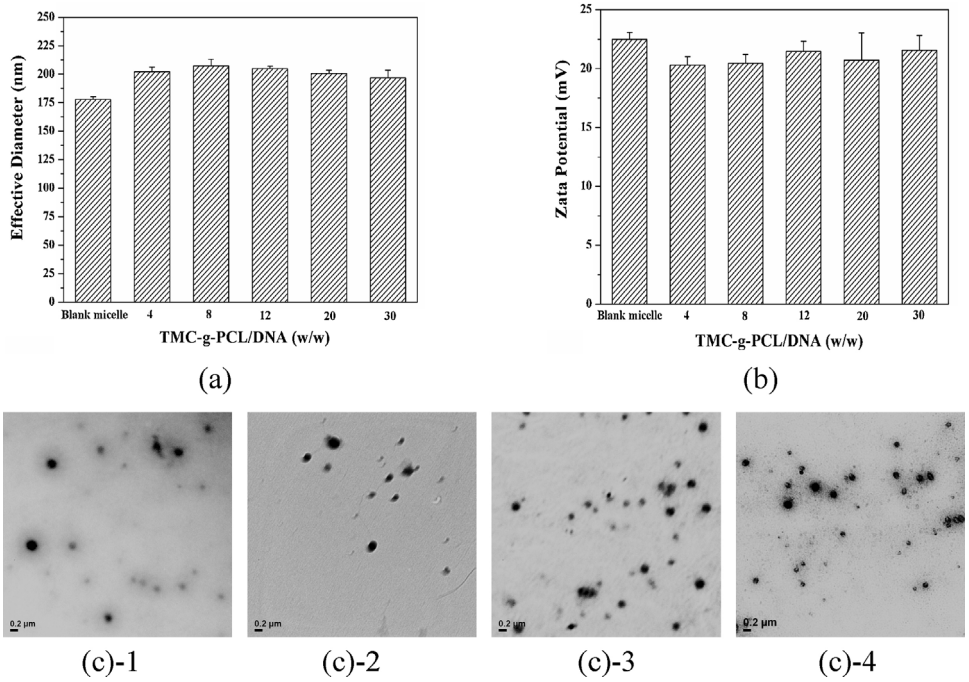

Fig. 2. The particle sizes (a) and zeta potentials (b) of TMC-g-PCL/DNA polyplexes; TEM micrographs of TMC-g-PCL blank nanoparticles ((c)-1), TMC-g-PCL/DNA-12 ((c)-2), TMC-g-PCL/DNA-20 ((c)-3) and TMC-g-PCL/DNA-30 ((c)-4) polyplexes.

polyplexes containing 2 μg FITC-DNA were added and incubated for 4 h. Then HEK293T cells were carefully washed three times with PBS in order to detach surface-associated polyplexes, trypsinized and resuspended in the medium. The efficiency of cell uptake was analyzed by flow cytometry (FCM, BD Bioscience). PEI/DNA polyplexes at an amino group to phosphate group ratio (N/P) of 8 were used as a control. All experiments were performed in triplicate. Error bars represent means ± SD for $n = 3$.

2.6.3. Intracellular distribution

For intracellular distribution, HEK293T cells were seeded into confocal imaging dishes at a density of 5×10^4 cells per dish. The TMC-g-PCL/DNA-30 polyplexes containing 4 μg FITC-DNA were added with chloroquine at the final concentration of 100 μM, cocultured with cells for 12 h. Then, the cells were washed five times with PBS, incubated with Lyso Tracker® Red DND-99 for 60 min. After that, the cells were washed five times with PBS, fixed with 4% (w/v) paraformaldehyde for 30 min and rinsed three times with PBS. Following incubation with DAPI for 15 min, the cells were washed three times with PBS. The intracellular distribution of polyplexes was analyzed by confocal laser scanning microscope (CLSM, Leica TSSP5, Germany). The polyplexes without chloroquine addition were investigated as a control.

2.6.4. In vitro transfection

The transfection efficiency assay used the green fluorescent protein (GFP) as the reporter protein. HEK293T cells were seeded in 24-well tissue culture plates at a density of 1×10^5 cells per well and incubated for 24 h prior to the transfection experiments. TMC-g-PCL/DNA polyplexes containing 2 μg pEGFP at different weight ratios with or without chloroquine were added to each well. The final concentration of chloroquine in each well was 100 μM. After incubation for 4 h, the media was replaced with fresh complete medium and incubated for further 44 h. Fluorescence spectroscopy was used to observe the expression of the green fluorescent protein (GFP). The transfection results were then measured by flow cytometry. PEI/DNA polyplexes at N/P ratio of 8 were used as a control. All transfection experiments were performed in triplicate.

3. Results and discussion

3.1. Characterization of TMC-g-PCL

The structure of TMC-g-PCL was characterized by ^{1}H NMR (Fig. 1). The degree of quaternization in TMC-g-PCL was 78.7%, as calculated from Eq. (1), where I_7 and I_8 were the peak areas of the protons from trimethyl amino groups and dimethyl amino groups respectively. PCL grafting level was calculated according to the Eq. (2), where I_e and I_1 were the integrated areas of the peaks at 2.21 and 5.25 ppm respectively. The grafting degree of PCL was 1.2%.

$$\text{Trimethylation degree} = \frac{I_7/9}{I_7/9 + I_8/6} \times 91.5\% \times 100\% \quad (1)$$

$$\text{PCL\%} = \frac{I_e}{2 \times 35 \times I_1} \times 100\% \quad (2)$$

The introduction of hydrophobic PCL moieties into TMC could induce the amphiphilicity-driven self association, which resulted in the formation of nanoparticles in an aqueous media. The critical aggregation concentration (CAC) of TMC-g-PCL was studied by fluorescence probe methods. Pyrene was used as a fluorescent probe because its vibrational fine structure was sensitive to polarity and it produced distinct excimer fluorescence under conditions of sufficiently high concentration and mobility (Zhou, Zhang, Chen, Guo, & Zhou, 2011). With an increase in TMC-g-PCL concentrations, the total fluorescent intensity I increased, and fluorescence spectrum shifted. A negligible change of intensity ratios was observed at a low concentration range. But the intensity ratios showed a sharp increase above a certain concentration, which indicated the incorporation of pyrene into the hydrophobic core region of the nanoparticles. The ratio I_{339}/I_{334} of the pyrene excitation spectra was used to determine CAC of TMC-g-PCL in water. The plot of the intensity ratio I_{339}/I_{334} of the pyrene excitation spectra against the logarithm of the different polymers concentrations was shown

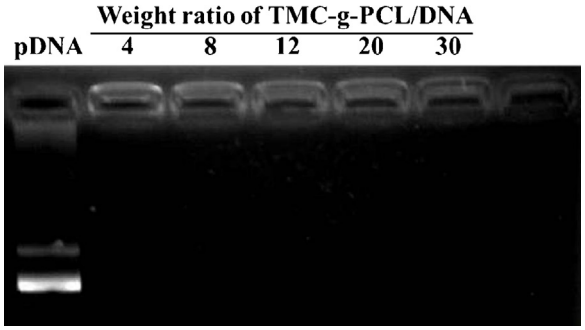

Fig. 3. Gel retardation assay for the pDNA binding ability of TMC-g-PCL nanoparticles. Numbers indicate the carrier/DNA weight ratio.

in Fig. 1B. By examining the (0, 0) band in the pyrene excitation spectrum and comparing the intensity ratio (I_{339}/I_{334}), CAC of TMC-g-PCL was about 0.02 mg/mL.

3.2. The property of TMC-g-PCL/DNA polyplexes

As shown in Fig. 2a, the average particle size of TMC-g-PCL blank nanoparticles was about 180 nm. The zeta potential was about 22 mV (Fig. 2b), which contributed to the positive charged TMC chains on the surface of the nanoparticles. Due to the electrostatic attraction, it could condense DNA and form polyplexes. By changing the weight ratios of TMC-g-PCL to DNA, different TMC-g-PCL/DNA polyplexes were then prepared. TMC-g-PCL/DNA polyplexes showed a narrow size distribution and a nearly constant average size of 200 nm when the weight ratio increased from 4 to 30. The zeta potential of TMC-g-PCL/DNA polyplexes was about 20 mV. As for particle size and zeta potential, there were negligible differences between TMC-g-PCL nanoparticles and TMC-g-PCL/DNA polyplexes probably owing to the utilization of excess amount of cationic TMC shell for the gene condensation. Transmission electron microscopic examination of TMC-g-PCL/DNA polyplexes revealed spherical morphology with diameters ranging from 100 to 200 nm (Fig. 2c), which was consistent with dynamic light scattering measurement.

DNA condensation ability was evaluated by gel retardation assay. As shown in Fig. 3, TMC-g-PCL nanoparticles achieved complete retardation of DNA at weight ratio from 4 to 30. It suggested a strong DNA binding ability of TMC-g-PCL. The effective gene condensation capacity may result from the increment of cationic charge densities due to the formation of nanoparticles in an aqueous environment. Furthermore, hydrophobic interactions between hydrophobic TMC moieties and charge-neutralized DNA segments were also accountable for the enhanced gene condensation capacity of TMC-g-PCL.

3.3. Aggregation study of polyplexes

The extracellular stability of polyplexes is of critical concern for gene delivery systems (Luo, Pan, Feng, Wen, & Zhang, 2010). In this case the stability of polyplexes was investigated by DLS by following the time-dependence of the particle size in physiological salt condition (Fig. 4). PEI/DNA polyplexes at N/P of 8 formed large aggregates quickly in physiological salt conditions. This was due to interparticle cross-bridging of polycations due to the reduced repulsive barriers. Compared with PEI/DNA polyplexes, the stability of TMC-g-PCL/DNA polyplexes was improved greatly. After 50 min incubation in physiological salt condition, the particle size of TMC-g-PCL/DNA-8 polyplexes increased from 280 nm to 380 nm. We speculate that by increasing the ionic strength of the solution, the affinity between nanoparticles and DNA chains

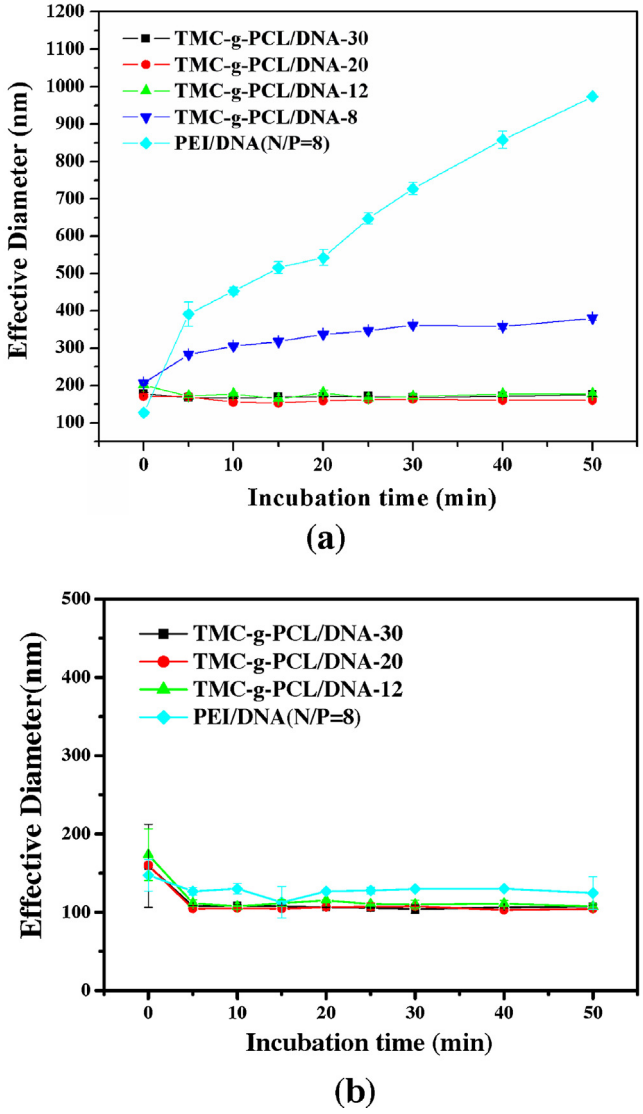

Fig. 4. The stability of TMC-g-PCL/DNA polyplexes in physiological salt condition (a) and in complete DMEM medium containing 10% FBS (b) determined by DLS. Error bars represent means ± SD for $n = 4$.

decreased and resulted in partial dissociation. However, the stability of TMC-g-PCL/DNA polyplexes at a weight ratio of 12, 20 and 30 was significantly improved. This could be due to the intermolecular hydrogen bonds among TMC segments. On the other hand, the increment of cationic charge densities on the micellar TMC-g-PCL nanoparticles could result in enhanced DNA binding ability. This may account for the excellent stability of polyplexes in physiological conditions.

The stability of TMC-g-PCL/DNA polyplexes in complete DMEM medium containing 10% fetal bovine serum was also evaluated by DLS. As shown in Fig. 4b, PEI/DNA and TMC-g-PCL/DNA polyplexes were stable. The size of gene polyplexes kept almost invariable during the incubation time, which was important in vivo application.

3.4. Cell toxicity

The cytotoxicity was measured by MTT viability assay. The results are shown in Fig. 5. For TMC-g-PCL/DNA and PEI/DNA polyplexes, cell cytotoxicity increased with the increment of weight ratio. PEI/DNA polyplexes with strong positive surface charge could disrupt the cell membrane and induce cell membrane toxicity.

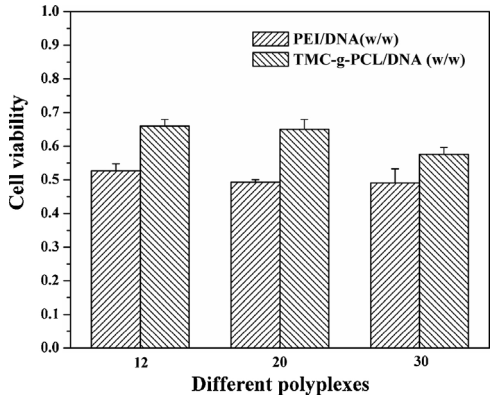

Fig. 5. The cytotoxicity of TMC-g-PCL/DNA polyplexes measured by MTT. Error bars represent the standard deviation of five measurements.

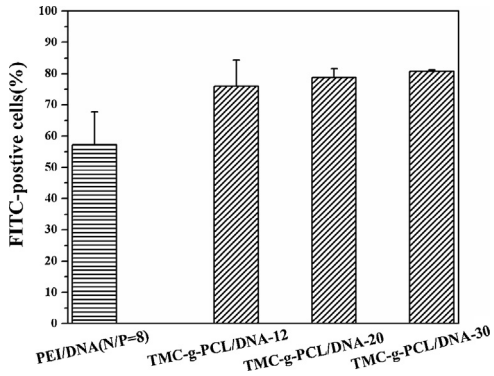

Fig. 6. Cell uptake efficiency after 4 h addition of TMC-g-PCL/DNA polyplexes in HEK293T cells determined by flow cytometry. PEI/DNA polyplexes at N/P of 8 were used as control. Error bars represent means ± SD for $n = 3$.

At the same weight ratio, TMC-g-PCL/DNA polyplexes showed lower cell cytotoxicity than PEI/DNA polyplexes. However, due to the trimethylated nature of TMC segments, TMC-g-PCL/DNA polyplexes showed less than 70% viability. This was a limitation of our delivery system.

3.5. Cell uptake and intracellular distribution

Endocytosis is one of the barriers that polyplexes must overcome for transfection (Sahay, Alakhova, & Kabanov, 2010). Many factors, such as particle size, zeta poteitial, polyplex stability in physiological media, have a great effect on the cell uptake. TMC-g-PCL/FITC-DNA polyplexes were added to HEK293T cells. After incubation 4 h, the uptake efficiency was determined by flow cytometry. Fig. 6 indicated the uptake efficiency of TMC-g-PCL/FITC-DNA polyplexes was higher than PEI/FITC-DNA polyplexes and reached about 80% at weight ratio of 30. It is well known that the positive charge density of polycation plays an important role in cell uptake. The TMC-g-PCL/FITC-DNA polyplexes with a positive-charged shell interacted easily with the negatively charged cell membrane. Moreover, the hydrophobic PCL modification might increase cell membrane–carrier interactions and/or destabilization of the cell membranes, leading to increased uptake efficiency.

Timely intracellular DNA unpacking and release is generally regarded as one of the important rate-limiting steps for nonviral condensing polycations. The most efficient gene polyplexes should have a subtle balance between polyplex stability to protect DNA against nucleases, and polyplex instability to permit DNA dissociation inside cells. CLSM was used to investigate the intracellular gene distribution. TMC-g-PCL/DNA-30 polyplexes were added and cocultured with cells for 12 h. Then the cells were washed by PBS and the lysosomes were stained to red fluorescence with Lyso Tracker® Red DND-99. The nuclei stained with DAPI were blue and DNA labeled with FITC was green. The confocal images in Fig. 7a showed that overlapping of red and green fluorescence in HEK293T

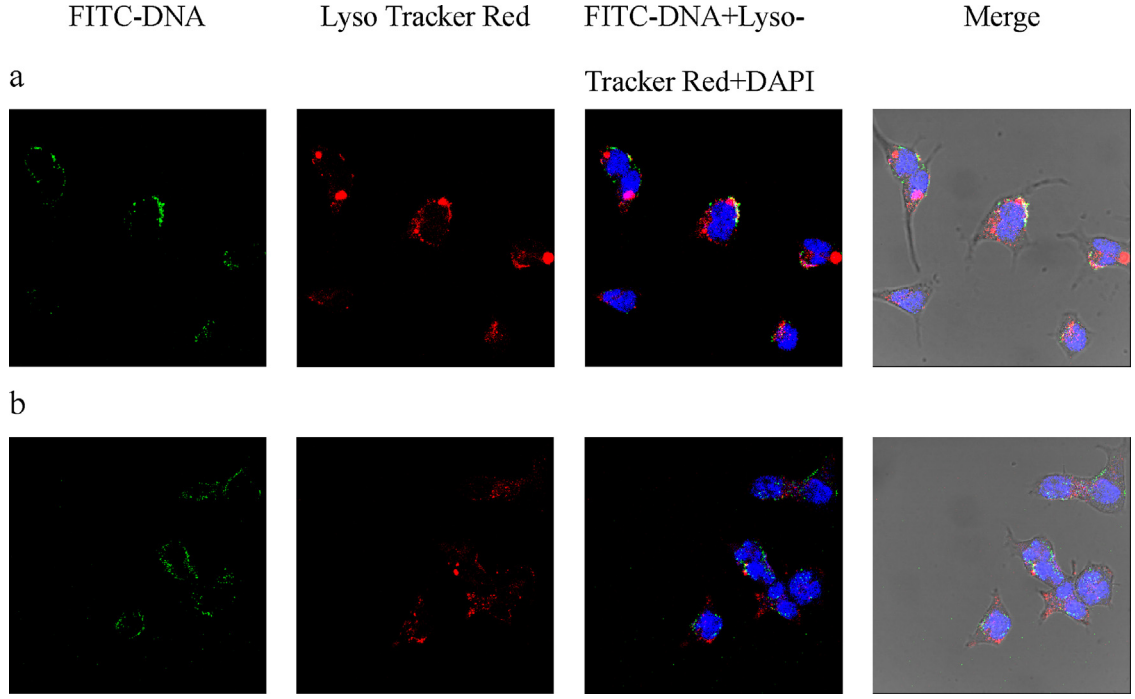

Fig. 7. Intracellular distribution of polyplexes without chloroquine (a) and with chloroquine (b) exposed to HEK293T cells approximately 12 h after incubation with the polyplexes. DNA was labeled with FITC (green), the nuclei were stained with DAPI (blue) and lysosomes of HEK293T were stained with Lyso Tracker Red (red). (For interpretation of the references to color in this figure legend, the reader is referred to the web version of the article.)

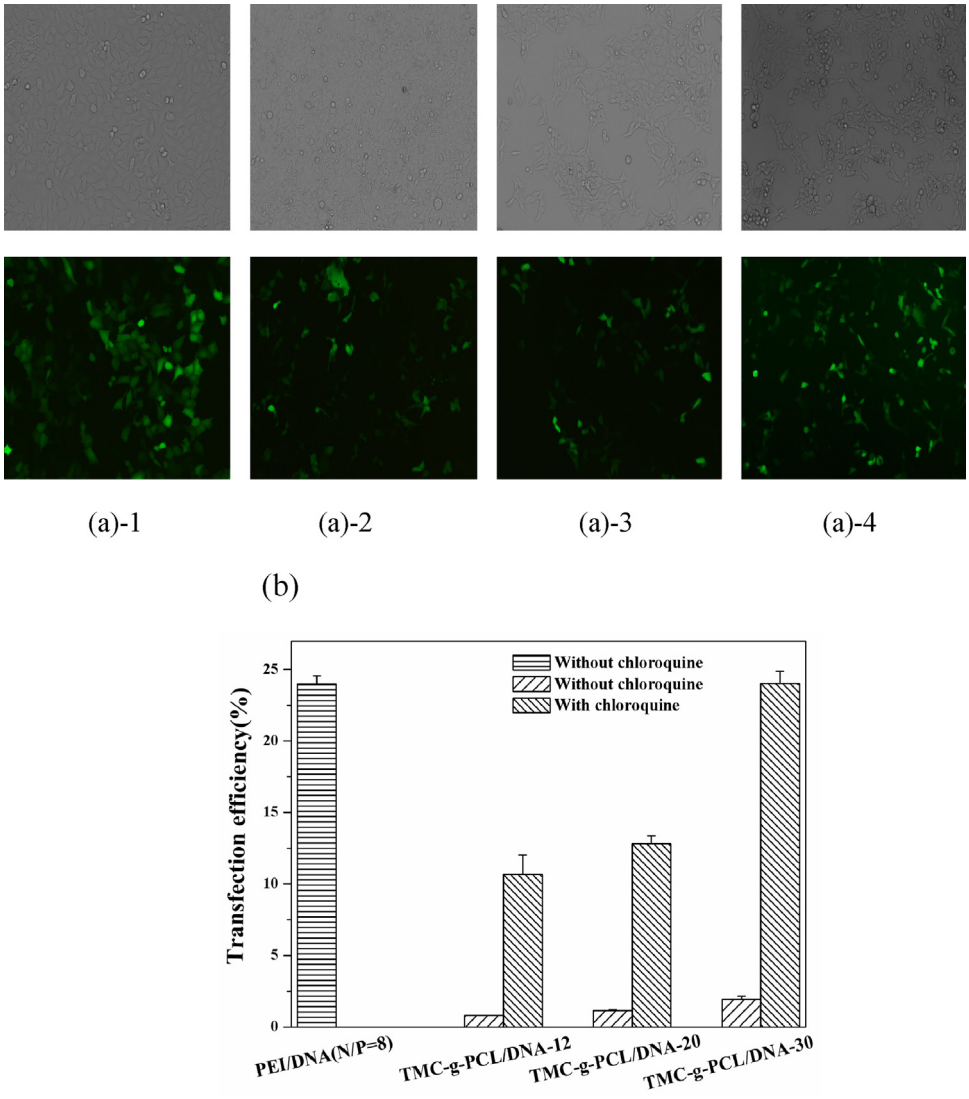

Fig. 8. The transfections of polyplexes to HEK293T cells measured by fluorescence microscopy (a) and flow cytometry (b). (a)-1 PEI/DNA; (a)-2 TMC-g-PCL/DNA-12 with chloroquine; (a)-3 TMC-g-PCL/DNA-20 with chloroquine; (a)-4 TMC-g-PCL/DNA-30 with chloroquine. PEI/DNA polyplexes at N/P of 8 were used as control. Error bars represent means ± SD for $n = 3$.

cells generated yellow stains in the merged images. It strongly demonstrated that TMC-g-PCL/DNA-30 polyplexes were mainly distributed in lysosome with little or no escape after incubation of 12 h. It was known that membrane destabilization and buffering capacity of the chitosan was originated by fairly low pK_a value (pK_a 6.0–6.5). However, due to high trimethylation degree, the buffering capacity of TMC-g-PCL was significantly reduced. On the other hand, the endosomal escape and pDNA release of chitosan-based polyplexes also depend on the degradation of chitosan molecular chains in endosome or lysosome vesicles (Koping-Hoggard et al., 2004; Liang et al., 2006; Pattani, Patravale, Panicker, & Potdar, 2009). Strong gene condensation and little or no lysosomal degradation of the polyplex for escape and weaken the polyplex may also account for the poor lysosomal escape of the TMC-g-PCL/DNA-30 polyplex.

Chloroquine has been proven to be an effective reagent to improve the transfection efficiency in several polycationic gene delivery systems (Choi, Liu, Park, & Kim, 1998; Mislick, Baldeschwieler, Kayyem, & Meade, 1995; Truong-Le et al., 1999), which was due to (i) pH buffering in endocytic vesicles, (ii) displacement of polycations from the nucleic acids in polyplexes, and (iii) alteration of the biophysical properties of the released nucleic acid. Fig. 7b indicated that with chloroquine, DNA was mainly distributed in cytoplasmic and some DNA even entered into nuclei. Such result demonstrated that chloroquine could effectively facilitate the lysosomal escape of polyplexes.

3.6. In vitro transfection

Fluorescence spectroscopy was used to observe the expression of the green fluorescent protein (GFP) in HEK293T cells after transfection 48 h (Fig. 8a). PEI polyplexes at N/P of 8 showed high transfection efficiency. The abundant primary and secondary amine groups provide PEI polyplexes with good proton buffering capacity, which facilitates the endosomal escape of PEI polyplexes and showed high transfection efficiency (Boussif et al., 1995). However, the transfection efficiency of TMC-g-PCL/DNA polyplexes alone was very low (Fig. 8b). Combining with the result of cell uptake and intracellular distribution, the TMC-g-PCL/DNA polyplexes might be endocytosed and transported into cells through an endo-lysosomal pathway. Lysosomal escape was one of the key rate-limiting steps for the transfection process. The low transfection of TMC-g-PCL/DNA polyplexes was mainly ascribed to the poor lysosomal escape. By adding chloroquine to exclude the above

limitation, the transfection efficiency was significantly improved. Such results confirmed that TMC-g-PCL/DNA polyplexes should effectively escape from lysosome and deliver DNA into the nuclei, which served as a prerequisite for efficient gene transcription. The degree of quaternization played an important role.

4. Conclusions

Trimethylated chitosan-g-poly(ε-caprolactone) was synthesized as gene vector. The degree of quaternization in TMC-g-PCL was 78.7% and grafting level of PCL was 1.2%. Owing to the amphiphilic character, TMC-g-PCL formed nanoparticles in aqueous media and the critical aggregation concentration was 0.02 mg/mL. Gel retardation assay indicated TMC-g-PCL nanoparticles could effectively condense DNA. TMC-g-PCL/DNA polyplexes showed a narrow size distribution and a nearly constant average size of 200 nm when weight ratio increased from 4 to 30. The zeta potential was about 22 mV. The polyplexes were stable in physiological salt conditions and in complete DMEM medium containing 10% fetal bovine serum. TMC-g-PCL/DNA polyplexes showed high uptake efficiency than PEI/DNA polyplexes. However, the transfection was quite low. The intracellular trafficking confirmed that high degree of quaternization influenced the buffer capacity of TMC-g-PCL and led to a reduction in the release from the lysosomes. By adding chloroquine to exclude the limitation of lysosome escape, the transfection efficiency of TMC-g-PCL/DNA polyplexes was similar to that of PEI/DNA polyplexes. The most efficient gene polyplexes should have a subtle balance between polyplex stability to protect DNA against nucleases, and polyplex instability to permit DNA dissociation inside cells. The degree of quaternization played an important role in TMC-based gene delivery system. Thereby, TMC-g-PCL with some modification to realize intracellular dissociation of DNA timely in relationship to lysosomal escape and reduce cytotoxicity, might have a promising application in non-viral gene therapy.

Acknowledgement

This work was financially supported by the National Natural Science Foundation of China (21074110 and 51273177).

References

Boussif, O., Lezoualc'h, F., Zanta, M. A., Mergny, M. D., Scherman, D., Demeneix, B., & Behr, J. P. (1995). A versatile vector for gene and oligonucleotide transfer into cells in culture and in vivo: Polyethylenimine. *Proceedings of the National Academy of Sciences*, *92*(16), 7297–7301.

Cai, G., Jiang, H., Tu, K., Wang, L., & Zhu, K. (2009). A facile route for regioselective conjugation of organo-soluble polymers onto chitosan. *Macromolecular Bioscience*, *9*(3), 256–261.

Chae, S. Y., Son, S., Lee, M., Jang, M.-K., & Nah, J.-W. (2005). Deoxycholic acid-conjugated chitosan oligosaccharide nanoparticles for efficient gene carrier. *Journal of Controlled Release*, *109*(1–3), 330–344.

Choi, Y. H., Liu, F., Park, J. S., & Kim, S. W. (1998). Lactose-poly(ethylene glycol)-grafted poly-L-lysine as hepatoma cell-targeted gene carrier. *Bioconjugate Chemistry*, *9*(6), 708–718.

Cook, S. E., Park, I. K., Kim, E. M., Jeong, H. J., Park, T. G., Choi, Y. J., Akaike, T., & Cho, C. S. (2005). Galactosylated polyethylenimine-graft-poly(vinyl pyrrolidone) as a hepatocyte-targeting gene carrier. *Journal of Controlled Release*, *105*(1–2), 151–163.

Drevelle, O., Daviau, A., Lauzon, M.-A., & Faucheux, N. (2013). Effect of BMP-2 and/or BMP-9 on preosteoblasts attached to polycaprolactone functionalized by adhesive peptides derived from bone sialoprotein. *Biomaterials*, *34*(4), 1051–1062.

Folmer, B. J. B., Sijbesma, R. P., Versteegen, R. M., van der Rijt, J. A. J., & Meijer, E. W. (2000). Supramolecular polymer materials: Chain extension of telechelic polymers using a reactive hydrogen-bonding synthon. *Advanced Materials*, *12*(12), 874–878.

Germershaus, O., Mao, S., Sitterberg, J., Bakowsky, U., & Kissel, T. (2008). Gene delivery using chitosan, trimethyl chitosan or polyethylenglycol-graft-trimethyl chitosan block copolymers: Establishment of structure–activity relationships in vitro. *Journal of Controlled Release*, *125*(2), 145–154.

Hu, F. Q., Zhao, M. D., Yuan, H., You, J., Du, Y. Z., & Zeng, S. (2006). A novel chitosan oligosaccharide–stearic acid micelles for gene delivery: Properties and in vitro transfection studies. *International Journal of Pharmaceutics*, *315*(1–2), 158–166.

Itaka, K., & Kataoka, K. (2009). Recent development of nonviral gene delivery systems with virus-like structures and mechanisms. *European Journal of Pharmaceutics and Biopharmaceutics*, *71*(3), 475–483.

Kean, T., Roth, S., & Thanou, M. (2005). Trimethylated chitosans as non-viral gene delivery vectors: Cytotoxicity and transfection efficiency. *Journal of Controlled Release*, *103*(3), 643–653.

Kim, D. H., & Rossi, J. J. (2007). Strategies for silencing human disease using RNA interference. *Nature Reviews Genetics*, *8*(3), 173–184.

Köping-Höggård, M., Mel'nikova, Y. S., Vårum, K. M., Lindman, B., & Artursson, P. (2003). Relationship between the physical shape and the efficiency of oligomeric chitosan as a gene delivery system in vitro and in vivo. *Journal of Gene Medicine*, *5*(2), 130–141.

Koping-Hoggard, M., Varum, K. M., Issa, M., Danielsen, S., Christensen, B. E., Stokke, B. T., & Artursson, P. (2004). Improved chitosan-mediated gene delivery based on easily dissociated chitosan polyplexes of highly defined chitosan oligomers. *Gene Therapy*, *11*(19), 1441–1452.

Lee, K. Y., Kwon, I. C., Kim, Y. H., Jo, W. H., & Jeong, S. Y. (1998). Preparation of chitosan self-aggregates as a gene delivery system. *Journal of Controlled Release*, *51*(2–3), 213–220.

Lee, D., Lockey, R., & Mohapatra, S. (2006). Folate receptor-mediated cancer cell specific gene delivery using folic acid-conjugated oligochitosans. *Journal of Nanoscience and Nanotechnology*, *6*(9–10), 2860–2866.

Li, W., Chen, L., Huang, Z., Wu, X., Zhang, Y., Hu, Q., & Wang, Y. (2011). The influence of cyclodextrin modification on cellular uptake and transfection efficiency of polyplexes. *Organic & Biomolecular Chemistry*, *9*(22), 7799–7806.

Liang, D. C., Liu, W. G., Zuo, A. J., Sun, S. J., Cheng, N., Guo, G., Zhang, J. Y., & Yao, K. D. (2006). Pre-deliver chitosanase to cells: A novel strategy to improve gene expression by endocellular degradation-induced vector unpacking. *International Journal of Pharmaceutics*, *314*(1), 63–71.

Lim Soo, P., Luo, L., Maysinger, D., & Eisenberg, A. (2002). Incorporation and release of hydrophobic probes in biocompatible polycaprolactone-block-poly(ethylene oxide) micelles: Implications for drug delivery. *Langmuir*, *18*(25), 9996–10004.

Liu, W. G., De Yao, K., & Liu, Q. G. (2001). Formation of a DNA/N-dodecylated chitosan complex and salt-induced gene delivery. *Journal of Applied Polymer Science*, *82*(14), 3391–3395.

Liu, W., Sun, S., Cao, Z., Zhang, X., Yao, K., Lu, W. W., & Luk, K. D. K. (2005). An investigation on the physicochemical properties of chitosan/DNA polyelectrolyte complexes. *Biomaterials*, *26*(15), 2705–2711.

Liu, W. G., Zhang, X., Sun, S. J., Sun, G. J., Yao, K. D., Liang, D. C., Guo, G., & Zhang, J. Y. (2003). N-alkylated chitosan as a potential nonviral vector for gene transfection. *Bioconjugate Chemistry*, *14*(4), 782–789.

Lu, B., Wang, C.-F., Wu, D.-Q., Li, C., Zhang, X.-Z., & Zhuo, R.-X. (2009). Chitosan based oligoamine polymers: Synthesis, characterization, and gene delivery. *Journal of Controlled Release*, *137*(1), 54–62.

Luo, X., Pan, S., Feng, M., Wen, Y., & Zhang, W. (2010). Stability of poly(ethylene glycol)-graft-polyethylenimine copolymer/DNA complexes: Influences of PEG molecular weight and PEGylation degree. *Journal of Materials Science: Materials in Medicine*, *21*(2), 597–607.

Maji, S., Mitschang, F., Chen, L., Jin, Q., Wang, Y., & Agarwal, S. (2012). Functional poly(dimethyl aminoethyl methacrylate) by combination of radical ring-opening polymerization and click chemistry for biomedical applications. *Macromolecular Chemistry and Physics*, *213*(16), 1643–1654.

Mansouri, S., Cuie, Y., Winnik, F., Shi, Q., Lavigne, P., Benderdour, M., Beaumont, E., & Fernandes, J. C. (2006). Characterization of folate-chitosan-DNA nanoparticles for gene therapy. *Biomaterials*, *27*(9), 2060–2065.

Mao, S., Shuai, X., Unger, F., Wittmar, M., Xie, X., & Kissel, T. (2005). Synthesis, characterization and cytotoxicity of poly(ethylene glycol)-graft-trimethyl chitosan block copolymers. *Biomaterials*, *26*(32), 6343–6356.

Mislick, K. A., Baldeschwieler, J. D., Kayyem, J. F., & Meade, T. J. (1995). Transfection of folate-polylysine DNA complexes: Evidence for lysosomal delivery. *Bioconjugate Chemistry*, *6*(5), 512–515.

Mosmann, T. (1983). Rapid colorimetric assay for cellular growth and survival: Application to proliferation and cytotoxicity assays. *Journal of Immunological Methods*, *65*(1–2), 55–63.

O'Connor, T. P., & Crystal, R. G. (2006). Genetic medicines: Treatment strategies for hereditary disorders. *Nature Reviews Genetics*, *7*(4), 261–276.

Park, Y. K., Park, Y. H., Shin, B. A., Choi, E. S., Park, Y. R., Akaike, T., & Cho, C. S. (2000). Galactosylated chitosan–graft–dextran as hepatocyte-targeting DNA carrier. *Journal of Controlled Release*, *69*(1), 97–108.

Pattani, A., Patravale, V. B., Panicker, L., & Potdar, P. D. (2009). Immunological effects and membrane interactions of chitosan nanoparticles. *Molecular Pharmaceutics*, *6*(2), 345–352.

Peng, Q., Chen, F., Zhong, Z., & Zhuo, R. (2010). Enhanced gene transfection capability of polyethylenimine by incorporating boronic acid groups. *Chemical Communications (Cambridge, England)*, *46*(32), 5888–5890.

Pires, L. R., Oliveira, H., Barrias, C. C., Sampaio, P., Pereira, A. J., Maiato, H., Simoes, S., & Pego, A. P. (2011). Imidazole-grafted chitosan-mediated gene delivery: In vitro study on transfection, intracellular trafficking and degradation. *Nanomedicine*, *6*(9), 1499–1512.

Ren, K., Ji, J., & Shen, J. (2005). Tunable DNA release from cross-linked ultrathin DNA/PLL multilayered films. *Bioconjugate Chemistry*, *17*(1), 77–83.

Sahay, G., Alakhova, D. Y., & Kabanov, A. V. (2010). Endocytosis of nanomedicines. *Journal of Controlled Release*, *145*(3), 182–195.

Sang Yoo, H., Eun Lee, J., Chung, H., Chan Kwon, I., & Young Jeong, S. (2005). Self-assembled nanoparticles containing hydrophobically modified glycol chitosan for gene delivery. *Journal of Controlled Release*, *103*(1), 235–243.

Sato, T., Kawakami, T., Shirakawa, N., & Okahata, Y. (1995). Preparation and characterization of DNA–lipoglutamate complexes. *Bulletin of the Chemical Society of Japan*, *68*(9), 2709–2715.

Son, S., Chae, S., Choi, C., Kim, M.-Y., Ngugen, V., Jang, M.-K., Nah, J.-W., & Kweon, J. (2004). Preparation of a hydrophobized chitosan oligosaccharide for application as an efficient gene carrier. *Macromolecular Research*, *12*(6), 573–580.

Truong-Le, V. L., Walsh, S. M., Schweibert, E., Mao, H.-Q., Guggino, W. B., August, J. T., & Leong, K. W. (1999). Gene transfer by DNA–gelatin nanospheres. *Archives of Biochemistry and Biophysics*, *361*(1), 47–56.

Varum, K. M., Ottoy, M. H., & Smidsrod, O. (1994). Water-solubility of partially N-acetylated chitosans as a function of pH: Effect of chemical composition and depolymerisation. *Carbohydrate Polymers*, *25*(2), 65–70.

Verheul, R. J., Amidi, M., van der Wal, S., van Riet, E., Jiskoot, W., & Hennink, W. E. (2008). Synthesis, characterization and in vitro biological properties of O-methyl free N,N,N-trimethylated chitosan. *Biomaterials*, *29*(27), 3642–3649.

Wang, Y., Zhu, Y., Hu, Q., & Shen, J. (2008). Construction of caged polyplexes with a reversible intracellular unpacking property to improve stability and transfection. *Acta Biomaterialia*, *4*(5), 1235–1243.

Wei, X., Gong, C., Shi, S., Fu, S., Men, K., Zeng, S., Zheng, X., Gou, M., Chen, L., Qiu, L., & Qian, Z. (2009). Self-assembled honokiol-loaded micelles based on poly(ε-caprolactone)–poly(ethylene glycol)–poly(ε-caprolactone) copolymer. *International Journal of Pharmaceutics*, *369*(1–2), 170–175.

Yu, H., Chen, X., Lu, T., Sun, J., Tian, H., Hu, J., Wang, Y., Zhang, P., & Jing, X. (2007). Poly(L-lysine)-graft-chitosan copolymers: Synthesis, characterization, and gene transfection effect. *Biomacromolecules*, *8*(5), 1425–1435.

Zhang, H., Cai, G., Tang, G., Wang, L., & Jiang, H. (2011). Synthesis, self-assembly, and cytotoxicity of well-defined trimethylated chitosan-O-poly(ε-caprolactone): Effect of chitosan molecular weight. *Journal of Biomedical Materials Research Part B: Applied Biomaterials*, *98B*(2), 290–299.

Zhou, Q., Zhang, Z., Chen, T., Guo, X., & Zhou, S. (2011). Preparation and characterization of thermosensitive pluronic F127-b-poly(ε-caprolactone) mixed micelles. *Colloids and Surfaces B: Biointerfaces*, *86*, 45–57.